GEOLOGICA BELGICA (2012) 15/3: 126-136

Geometry and kinematics of the low-grade metamorphic 'Herbeumont shear zone' in the High-Ardenne slate belt (Belgium)

Yvonne A. SCHAVEMAKER[1,2], Johannes H.P. DE BRESSER[1], Hervé VAN BAELEN[2] & Manuel SINTUBIN[2,*]

[1]*Faculty of Geosciences, Department of Earth Sciences, Utrecht University, The Netherlands*
[2]*Geodynamics & Geofluids Research Group, Department of Earth & Environmental Sciences, K.U.Leuven, Celestijnenlaan 200E, B-3001 Leuven, Belgium*
** corresponding author: manuel.sintubin@ees.kuleuven.be*

ABSTRACT. On the geological maps of the High-Ardenne slate belt (Belgium) an EW-trending, weakly S-dipping thrust fault is classically drawn, bordering the Eifel depression to the south. The 'type locality' of this fault lies in a – now completely overgrown – railway section at Herbeumont. This fault is indeed known as the 'Herbeumont fault'. A detailed structural and microstructural analysis of an outcrop area on the east bank of the Semois river, south of the railway section, allowed us to complement the geometrical and kinematic context of the classical 'Herbeumont fault'. The rocks exposed are predominantly fine-grained siliciclastic rocks belonging to the Lower Devonian.
Besides the bedding (S_0), which is often very difficult to discern, three types of tectonic foliation can be distinguished: a primary cleavage (S_1) at small angle to the bedding, a shear band foliation (SBF = S_2) and an axial-planar, crenulation cleavage (S_3) of late, shear-related folds affecting all pre-existing structural features. The pervasiveness – or even the mere presence – of these foliations is highly dependent on lithology, layer thickness and competence contrast within the multilayer sequence, even to the degree that a strongly developed shear band foliation can easily be mistaken as bedding. Other typical structural features include folded, boudinaged layers and folded, foliation boudins, as well as chevron folds.
All these structural features can be fitted in a kinematic model of a single, polyphase progressive top-to-the-north shearing event, occurring in the late stages of the Variscan orogeny. The outcrop area studied thus offers an excellent look into a low-grade metamorphic shear zone – the 'Herbeumont shear zone' – that developed in mid-crustal, brittle-plastic deformation conditions in a slate belt. Evidence of purely brittle thrust faulting – the 'Herbeumont fault' – could, however, not be identified in the outcrop area studied.

KEYWORDS: progressive deformation, shear zone, slate belt, multiple foliations, folded boudins, Variscan

1. Introduction

Multiple foliations in metamorphic crystalline rocks are commonly considered diagnostic of a shear zone (cf. Passchier & Trouw 2005, Trouw et al. 2010). In mylonites we find the characteristic S-C fabrics (Berthé et al. 1979, Passchier & Trouw 2005) and C' fabrics (Passchier & Trouw 2005, Platt & Vissers 1980). In a slaty environment, on the other hand, multiple cleavages are often seen as indicative of multiple deformation events or even multiple orogenic events affecting the low-grade, fine-grained siliciclastic series (Passchier & Trouw 2005).

In the context of the High-Ardenne slate belt, multiple cleavage development in the Lower Palaeozoic basement inliers (e.g. Stavelot-Venn, Rocroi) has indeed been seen as evidence of an older, pre-Variscan orogenic event (e.g. Belanger 1998, Delvaux de Fenffe & Laduron 1984, 1991, Geukens 1969). A study of multiple crenulation cleavages, present in the Ordovician (Salmian) slates in the southern part of the Stavelot-Venn inlier (Piessens & Sintubin 1997), demonstrates, however, that applying a single progressive, non-coaxial shear deformation can explain the presence of multiple crenulation cleavages, thus questioning its value as evidence in favour of an early, pre-Variscan orogenic event (Sintubin et al. 2009). Also in the Lower Devonian rocks in the core of the Eifel depression (Cugnon-Herbeumont region), multiple crenulation and kink generations have long been recognized (Fourmarier 1944, 1966, Fourmarier et al. 1968, Rondeel 1971). Because these rocks are only affected by the Late Carboniferous, Variscan orogeny, these multiple foliations need to be explained by a single, progressive deformation event.

The outcrop area along the banks of the Semois river, which is the subject of this paper, is located on the supposed trace of the 'Herbeumont fault', as coined by Fourmarier (1914) along the, at that time, newly excavated railway in the centre of Herbeumont. A detailed structural analysis of the outcrops, combined with a microfabric analysis on thin sections, reveals the

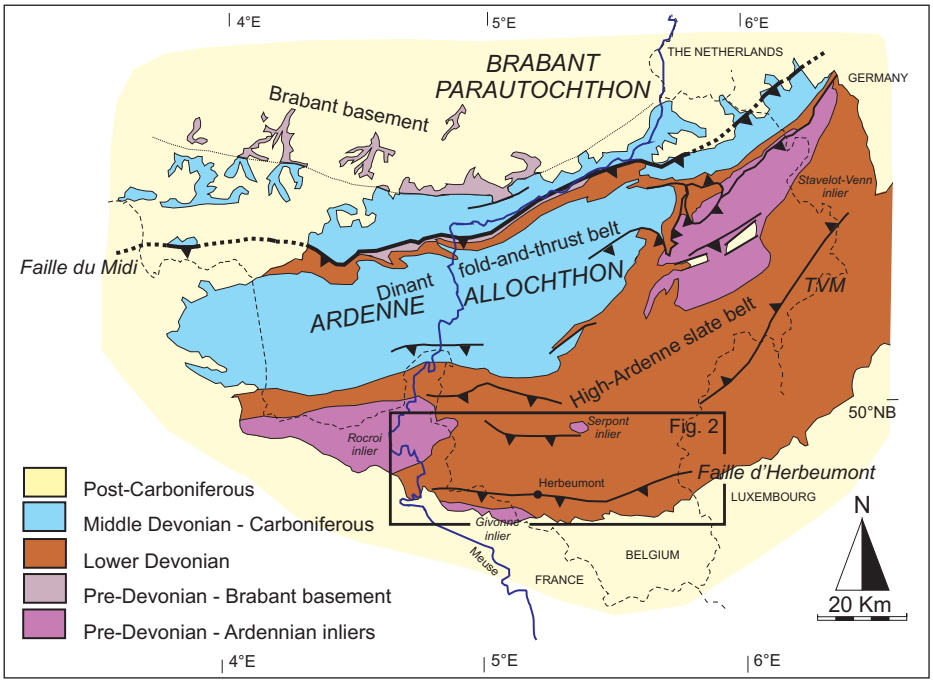

Figure 1. Simplified geological map of the Ardenne-Eifel area with indication of the main tectonostratigraphical entities. TVM: Trois-Vierges Malsbenden backthrust (after Sintubin et al. 2009).

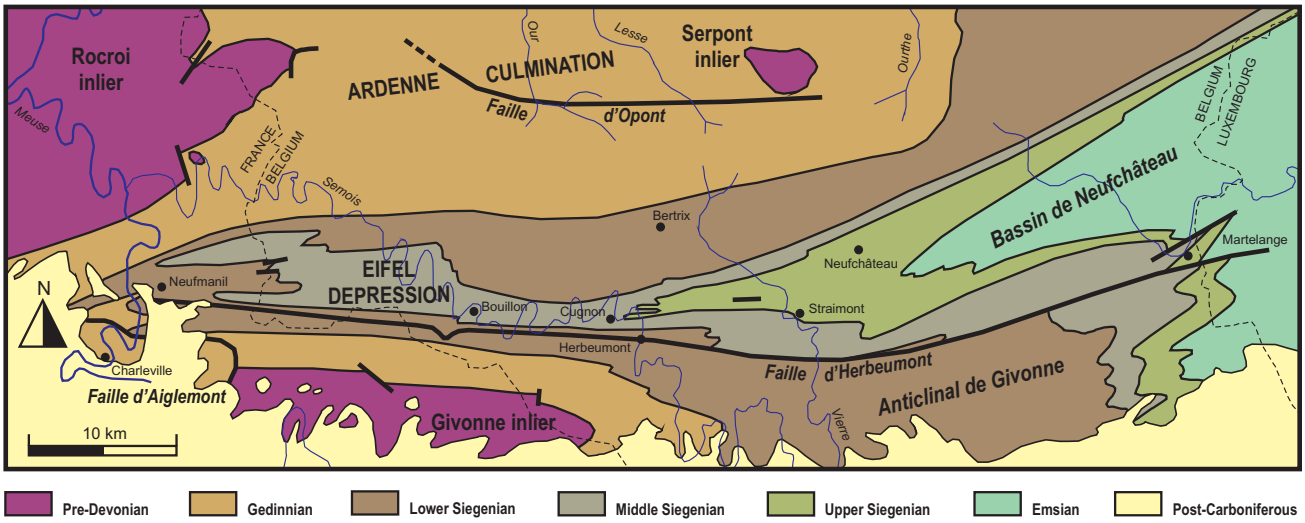

Figure 2. Simplified geological map of the western part of the High-Ardenne slate belt according to Asselberghs (1946), representing the region in which the 'Herbeumont fault' (*'Faille de Herbeumont'*) has been mapped (see figure 1 for location). In italic are indicated the original names (in French) of tectonostratigraphical entities and faults according to Asselberghs (1946). The 'old' Lower Devonian stratigraphy is used: 'Gedinnian' largely coincides with the Lochkovian; 'Siegenian' with the Pragian; and 'Emsian' with the Emsian.

presence of multiple foliations, boudin structures and chevron folds. In this paper, we present a kinematic model, explaining the complex superposition of all structural features. The inferred polyphase, progressive strain accumulation fits in an overall top-to-the-north shear context. The high-strain zone, exposed in the outcrop area, can thus be defined as the 'Herbeumont shear zone'. No purely brittle deformation, i.e. the 'Herbeumont fault', has been identified. The kinematic model allows to reflect on the nature of low-grade metamorphic shear zones in slate belts. It furthermore contributes to an improved understanding of the overall Variscan geodynamics of the High-Ardenne slate belt.

2. Geological setting

The High-Ardenne slate belt (HASB) forms the southernmost exposed domain in the Ardenne-Eifel area (France, Belgium, Luxembourg, Germany) of the Ardenne allochthon (Fig. 1), part of the Rhenohercynian foreland fold-and-thrust belt (Oncken et al. 1999), which is located at the northern extremity of the Central European Variscides. The HASB is composed of siliciclastic, predominantly argillaceous rock formations of early Devonian age. Largely, these relatively incompetent rock formations controlled the Variscan deformation, which eventually led under low-grade metamorphic conditions to the development of a slaty cleavage, the dominant structural feature in the HASB. This thick, Lower Devonian sequence reflects the rapid syn-rift basin fill, particularly active during the Pragian (Oncken et al. 1999), in the northern part of the developing Rhenohercynian ocean. Deformation in the HASB took place during the late Visean-early Serpukhovian – Sudetic – stage of the Variscan orogeny (Fielitz & Mansy 1999, Piqué et al. 1984). Greenschist-facies metamorphism is recorded in the Lower Devonian metasediments in the central part of the HASB (Beugnies 1986). This metamorphism is believed to be pre- to early synkinematic with respect to the prograding Variscan deformation and is considered to primarily have a burial origin (Fielitz & Mansy 1999). These metamorphic conditions persisted during the Variscan orogeny.

The HASB is structurally composed of the Ardenne culmination and the Eifel depression (Fig. 2). The Ardenne culmination involves predominantly siliciclastic metasediments of Lochkovian age. A number of Lower Palaeozoic basement inliers, i.e. the Rocroi and Serpont inliers in the west and the Stavelot-Venn inlier in the east, forms the backbone of the Ardenne culmination (Fig. 1). The predominantly siliciclastic metasediments in these basement inliers are Cambrian to middle Ordovician in age, and possibly reflect an early Palaeozoic rift basin development (Verniers et al. 2002). The existence of a pre-Variscan deformation event – the so-called Ardennian event – remains to date a matter of debate (Sintubin et al. 2009).

The Eifel depression – 'Bassin de Neufchâteau' according to Asselberghs (1946) – consists of Lower Devonian siliciclastic metasediments. In the west, the outcropping metasediments are of Pridolian to Pragian age, while towards the north-east the outcropping metasediments progressively young up to the Emsian and Eifelian. The Eifel depression shows an overall synformal architecture (Asselberghs 1946). The western part of the Eifel depression (Fig. 2) is rather narrow. It trends EW and is nearly horizontal to weakly E-plunging. To the south, it is bordered by the Givonne culmination – 'Anticlinal de Givonne' according to Asselberghs (1946) – with the Lower Palaeozoic

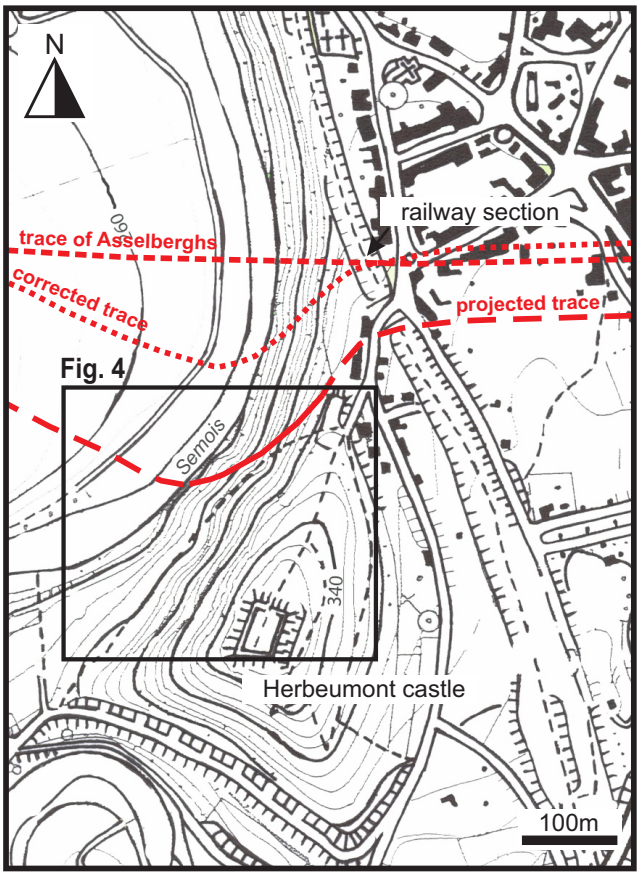

Figure 3. The study area at Herbeumont, indicating three traces of the 'Herbeumont fault': (a) the straight trace as on the map of Asselberghs (1946) (i.e. 'trace of Asselberghs'); (b) the corrected trace taking into account a 45°S dip of the fault starting from the 'type locality' in the railway section (i.e. 'corrected trace'); (c) the trace as we would expect based on the identification of the 'Herbeumont shear zone' (see figures 4 & 11) (i.e. 'projected trace').

Givonne inlier in its core (Fig. 2). The 'Herbeumont fault', as outlined by Asselberghs (1946), is commonly considered to separate both latter tectonostratigraphic entities.

The 'Herbeumont fault' – 'faille de Herbeumont' – has first been described by Fourmarier (1914) along the, at that time, newly excavated railway in the centre of Herbeumont (Fig. 3). He recognised an intensely disrupted and folded zone and supposed that this fault is the eastern continuation of the Aiglemont fault, described by Gosselet (1888) close to Charleville-Mézières (Fig. 2). In 1922 more evidence of a similar fault (e.g. folds, brecciation, veins, slickensides) was observed between Bouillon and Straimont (Asselberghs 1922). Asselberghs (1946) described the key elements of the 'Herbeumont fault' in the Herbeumont railway section: S-verging staircase folds in the footwall of the fault; 'crushed' slates in the direct footwall of the fault; and overturned N-verging folded and faulted quartzite layers intercalated in the slates in the hanging wall of the fault. The 'Herbeumont fault' itself – situated 50 m north of the viaduct – dips 45° to the south. The trace of the fault is speculated to extend towards Martelange in the east (Fig. 2). In total, Asselberghs (1946) described 10 localities along the Belgian trace of the fault, based on structures such as fault-related folds, brecciation, veins, slickensides.

The EW-running trace of 'Herbeumont fault' can thus be followed over a distance of more than 75 km from Charleville-Mézières to Martelange, passing through Bouillon and Herbeumont (Asselberghs 1946) (Fig. 2). The influence of the fault is supposed to be visible up to 2 km north of the fault (footwall). The overall dip of the fault varies from 45°S (Herbeumont), down to 15°S (Bouillon) and even 10°S (Neufmanil). The overall horizontal displacement is estimated to be at least 2500 m (Asselberghs 1946).

The 'Herbeumont fault' at its 'type locality' – the railway section at Herbeumont – separates metasediments of the same stratigraphical formation, i.e. the Anlier Formation sensu Asselberghs (1946). This formation belongs to the old 'Siegenian 1'. In the current Lower Devonian stratigraphy the metasediments exposed at Herbeumont most probably belong to the Mirwart Formation (Bultynck & Dejonghe 2001, Godefroid et al. 1994), of Lochkovian-Pragian age.

The 'straight' trace of the 'Herbeumont fault' on the map of Asselberghs (1946) (Fig. 2) is in conflict with its shallow southern dip, in particular taking into account the pronounced relief in the Semois valley region. At Herbeumont, we corrected the trace taking into account a 45°S dip starting from the – now completely overgrown and inaccessible – 'type locality' in the

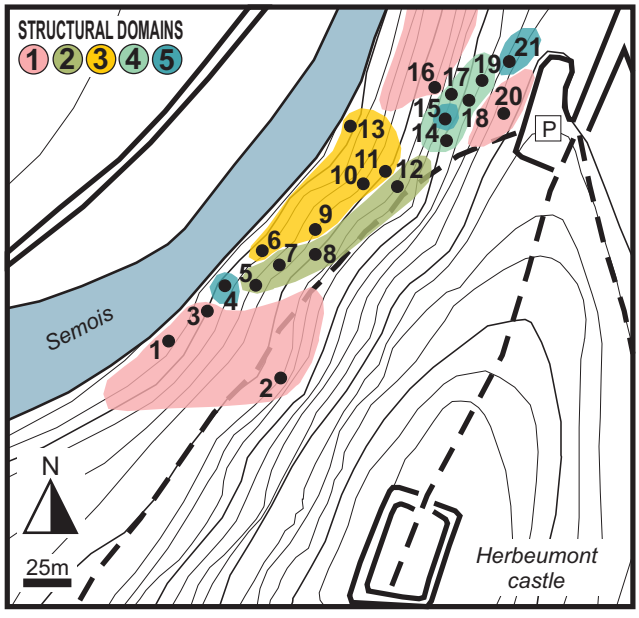

Figure 4. Detailed map of the outcrop area west of the Herbeumont castle (see figure 3 for location). All individual outcrops studied are indicated. The colour code indicates the structural domains (see text for further explanation) to which each of the individual outcrops has been assigned (see also figure 11).

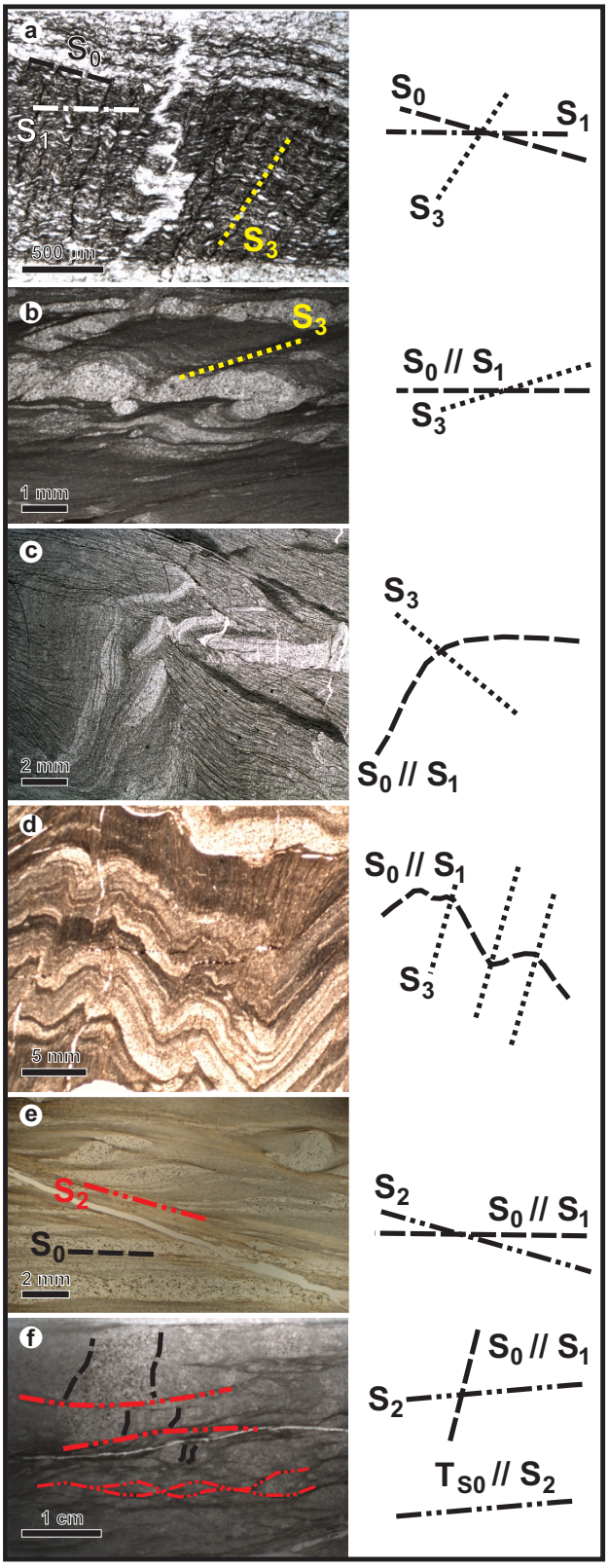

Figure 5. Micrographs illustrating the microstructural relationship between the different foliations. (a) small angle between bedding (S_0) and primary cleavage (S_1) is still observable; the latter has been affected by the crenulation cleavage S_3 (outcrop 17 – structural domain 4). (b) pinch-and-swell structure of mm-sized silty layers in multilayer sequence affected by the tertiary cleavage S_3 (outcrop 14 – structural domain 4). (c) fragmented layering in the core of an chevron fold, related to the tertiary cleavage S_3 (outcrop 15 – structural domain 5). (d) multilayer sequence affected by the crenulation cleavage S_3 (outcrop 15 – structural domain 5). (e) shear band foliation (SBF = S_2), fragmenting the primary composition layering, resulting in 'stretched fishes' (sample taken 600 m north of the study area – structural domain 2). (f) in the upper part of the thin section the primary compositional layering is dismembered by the SBF (S_2); in the lower part of the thin section the primary layering is completely transposed by the SBF (T_{S0} // S_2) (outcrop 13 – structural domain 3).

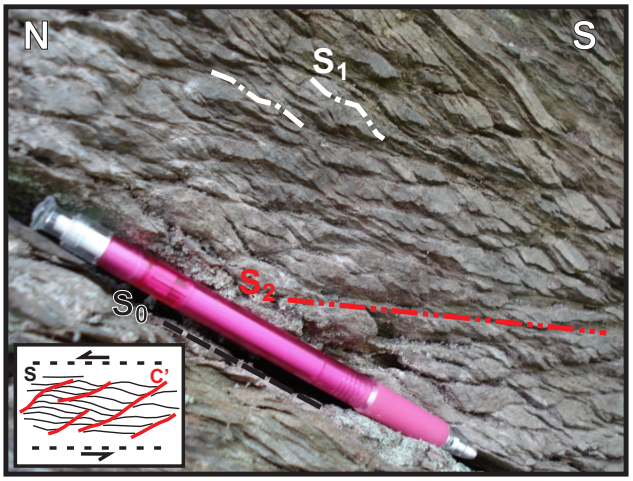

Figure 6. Detailed outcrop view of the shear band foliation (SBF = S_2), affecting the primary cleavage (S_1) sub-parallel to bedding (S_0) (outcrop 5 – structural domain 2) (pencil = ~15 cm). Bedding and primary cleavage is dipping ~30°S (see pencil); shear band foliation (S_2) is dipping ~16°S. This SBF (S_2) can easily be mistaken as bedding. Inset: extensional shear band foliation or C'-foliation in relation to overall shear movement (Passchier & Trouw 2005).

railway section to the west into the deeply incised Semois river valley. The 'Herbeumont fault' should subsequently be exposed in the outcrops on the east bank of the Semois river just northwest of the Herbeumont castle ('Forteresse d'Herbeumont') (Fig. 3).

Our research focused on this outcrop area, allowing us to study the geometry and kinematics of the 'Herbeumont fault'. In total 21 individual outcrops have been studied, spread mainly over an area extending ~300 m along the Semois river and over 60 m height difference from river level (~260 m) and the top of the ridge (~320 m) (Fig. 4). The rocks exposed in the outcrop area primarily consist of fine-grained, siliciclastic metasediments, ranging from greenish-grey mudstones to siltstones. Intercalated in these fine-grained rocks we find well-foliated layers of coarser-grained, creamy to grey, metasandstones – classically described as psammites by Belgian geologists.

3. Structural analysis

On the different outcrops a number of specific structural fabric elements have been identified. Besides the original bedding (S_0), three different tectonic foliations could be recognised (S_1, S_2, S_3), as well as folds and boudin structures. It should be noticed that each structural fabric element is not present in each (part of an) outcrop. Presence or absence is clearly controlled by the lithological composition. Based on the presence or absence of structural fabric elements, the outcrops have been grouped in a number of structural domains (Figs 4 & 11).

3.1 Bedding S_0

The original bedding (S_0) is only obvious in (parts of) the outcrops in which a lithological contrast is clearly observable (e.g. outcrops 14, 15, 17, 18, 19; Fig. 4). Multilayer sequences consist of an alternation of psammitic sandstones, siltstones and pelites. The psammitic layers are often dominant (up to 80%) in the multilayer sequence. Thicknesses of the individual psammitic layers range from mm- to cm-size (up to 10 cm). Multilayer psammitic packages, intercalated with very thin layers of pelitic material, up to 50 cm thickness can be observed. Often, these multilayer sequences are folded (e.g. outcrop 15) (Fig. 5c & d; Fig. 8a). In parts where the lithological contrast is not pronounced, bedding is no longer apparent on outcrop, in particular with respect to the other foliations. These sediments primarily consist of rather homogeneous, often finely laminated, siltstones and pelites (Fig. 7).

In thin section, traces of the original bedding can be recognised. Progressively, primary compositional layering (Fig. 5a & b) is, however, dismembered in isolated fragments (Fig. 5c), going from 'lensoid' fragments ('stretched fishes'), which still allow to identify the overall bedding attitude (Fig. 5e) at an angle to one of the tectonic foliations, to completely transposed, isolated fragments in a pelitic matrix (Fig. 5f). In the latter case, it is not possible anymore to identify the original bedding attitude based on the transposed bedding (T_{S0}) (Fig. 5f).

3.2 Primary cleavage S_1

Where bedding can be clearly identified in multilayer sequences, a primary cleavage (S_1) becomes apparent in the more pelitic parts of the sedimentary sequence. This primary cleavage shows a very small angle with respect to the bedding (up to 10°) (Fig. 5a). It is therefore fair to assume that, at those places where bedding cannot be identified unequivocally, the attitude of the primary cleavage may be used as a proxy of the original bedding attitude (Fig. 5b to f).

3.3 Shear band cleavage S_2

The dominant foliation, observed on the majority of the outcrops, can easily be mistaken in the field as bedding (Fig. 6), in particular

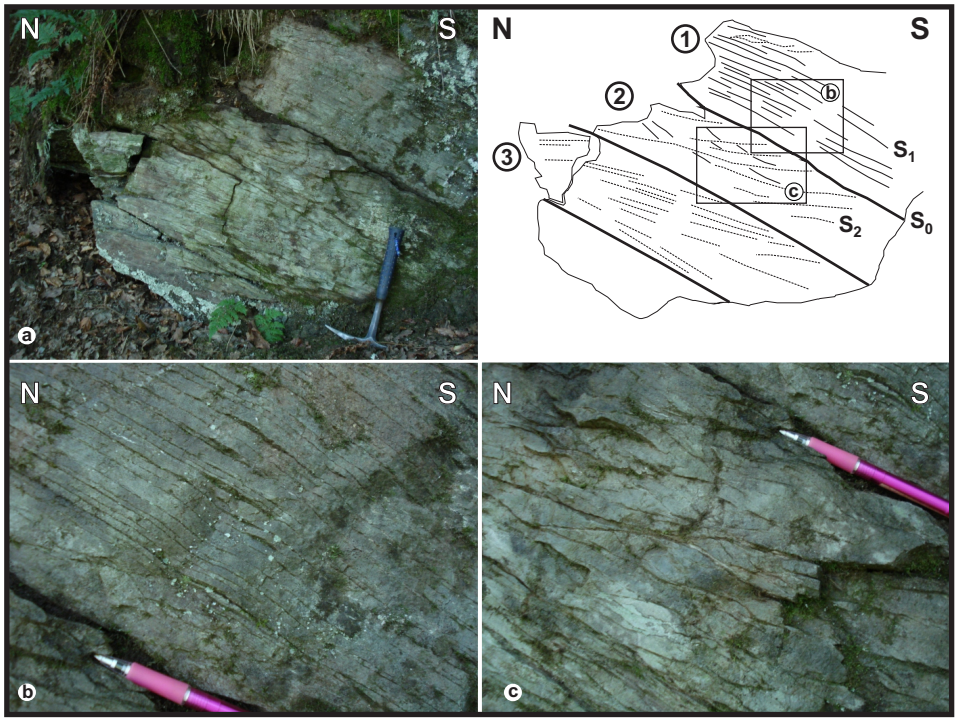

Figure 7. Lithology-dependence of the occurrence of tectonic foliations (outcrop 5 – structural domain 2). (a) photograph of outcrop (hammer = ~35 cm) and line drawing with indication of different foliations; notice the differences between layers 1 (psammitic composition), 2 (silty composition) and 3 (pelitic composition). (b) detailed view of layer 1 in which only the primary cleavage (S_1) is apparent (pencil = ~15 cm). (c) detailed view of layer 2 in which both SBF (S_2) and S_1 are observable (pencil = ~15 cm); in layer 3 only the SBF (S_2) is present. Between layers 2 and 3 the SBF (S_2) shows a typical cleavage refraction pattern.

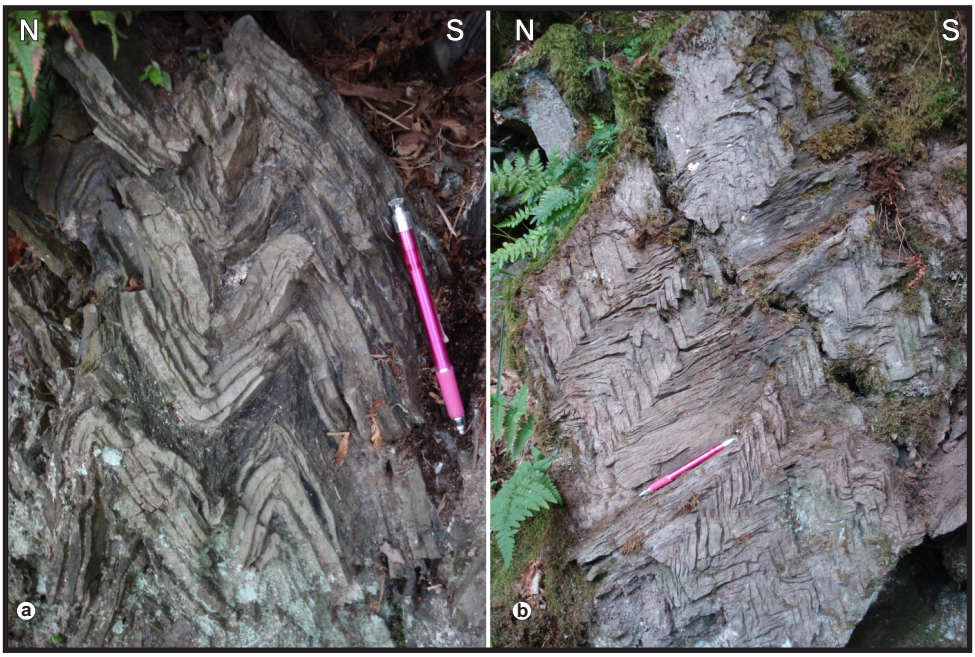

Figure 8. Chevron folds, associated with the tertiary cleavage S_3 (pencil = ~15 cm). (a) chevron folds affecting fine compositional layering (S_0) (outcrop 15 – structural domain 5). (b) chevron folds affecting the SBF (S_2) (outcrop 11 – structural domain 3); notice the thickness variation between both limbs (see also figure 9).

where this foliation is folded (Fig. 8b). This foliation is most obvious in the more silty, rather homogeneous parts of the outcrops (Fig. 7). It appears as a compositional layering, mimicking a primary sedimentary bedding. Where the foliation is not folded, it is weakly S-dipping (~10°S) to subhorizontal.

This tectonic foliation (S_2) clearly affects both the original bedding, where visible, and the primary cleavage (Fig. 5e). It causes the typical wavy appearance of the bedding (Fig. 6) due to minor dragging and shearing of the original bedding. Displacement along this secondary foliation can, however, become significant to the point that bedding can no longer be traced across this foliation (Fig. 5f). In the latter case, bedding seems completely transposed by the secondary foliation (i.e. T_{S0} // S_2).

This secondary foliation (S_2) shows all characteristics of an extensional shear band foliation (SBF) (Passchier & Trouw 2005, Platt & Vissers 1980), consistently indicating a top-to-the-north shearing. The SBF (S_2) does not occur in the psammitic layers of the metasedimentary sequence (e.g. outcrop 5 – Fig. 7b). In the more silty, finely laminated parts and in the pelitic horizons, the SBF (S_2) is clearly expressed, also showing cleavage refraction (e.g. outcrop 5 – Fig. 7c).

3.4 Folding and tertiary cleavage S_3

Two types of chevron folds have been identified. Both types have very similar outcrop characteristics: dm- to m-scale; upright to slightly N-verging; subvertical axial plane; subhorizontal to moderately plunging (~30°SE) NW-SE trending fold hinge lines. The difference between the two types lies in the nature of the folded foliation.

The first type of chevron folds developed in a multilayer sequence of mm- to cm-thick psammitic layers in predominantly pelitic series (e.g. outcrop 15 – Fig. 8a). The individual psammitic layers are discontinuous and show prominent thickness variation (ranging from a few mm to a few cm), indicative of boudinage. The folded foliation is definitively the bedding (S_0). In the more pelitic parts of the folded multilayer sequence a clear axial planar cleavage developed. In this type of folds, the prominent tertiary cleavage (S_3) is a compressional crenulation cleavage (Passchier & Trouw 2005) primarily affecting the primary cleavage fabric (S_1) in the pelitic horizons (Fig. 5a, c & d).

The second type of chevron folds affects the secondary cleavage (S_2) (e.g. outcrop 11 – Fig. 8b). Both symmetrical and asymmetrical chevrons have been observed. Typical for the

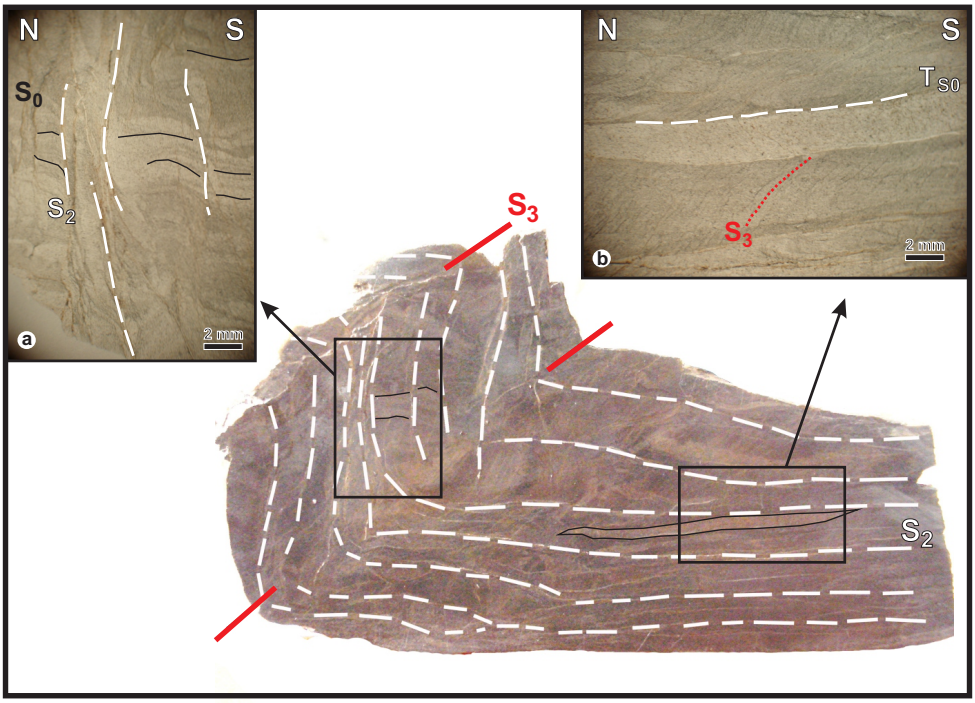

Figure 9
Detailed view of the hinge zone of a chevron fold affecting the SBF (S_2) (indicated by white dashed lines) (outcrop 11 – structural domain 3); compositional layering (S_0) is indicated by fine black lines; tertiary axial-planar cleavage (S_3) by red full line. (a) thin section of the 'thick' limb, in which bedding (S_0) can still be recognised at high angle to the SBF (S_2). (b) thin section of the 'thin' limb, in which bedding is completely transposed (T_{S0} // S_2).

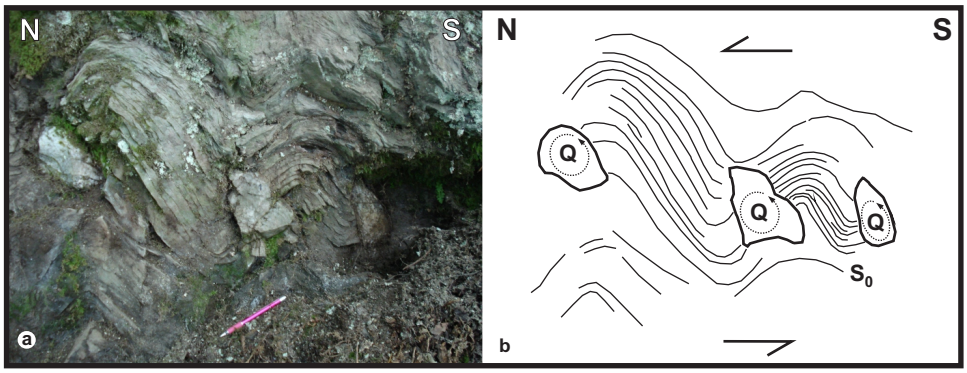

Figure 10. Train of folded boudins in highly foliated psammitic layers with quartz pods in the boudins necks (outcrop 15 – structural domain 5). (a) photograph of southern part of the outcrop (pencil = ~15 cm). (b) line drawing of folded layering (S_0) in between quartz pods (Q); the asymmetry of the flanking folds and internal rotation of the quartz pods fit a top-to-the-north shear strain.

asymmetrical chevron folds is the thickness variation between both limbs, as expressed by the microlithons in between the marked SBF (S_2). N-dipping limbs are consistently thinner than S-dipping limbs. In thin section it becomes clear that the thin limb is characterised by a bedding fabric that has been entirely transposed by the SBF (T_{S0} // S_2) (Fig. 9b); in the thick limb, on the other hand, bedding (S_0) can still be recognised at high angles to the SBF (S_2) (Fig. 9a). Also these chevron folds show an axial planar cleavage (S_3), most apparent as a crenulation of the secondary cleavage fabric (SBF = S_2) in the more pelitic horizons in the thin limb (Fig. 9b).

3.5 Boudinage

The individual, mm- to cm-thick, psammitic layers in the multilayer sequences are discontinuous and show prominent thickness variation (ranging from a few mm to a few cm), typical for pinch-and-swell structures (Fig. 5b). These pinch-and-swell structures indiscriminately occur in both limbs of the abovementioned chevron folds (Fig. 8a), clearly indicating that layer-parallel extension predates the folding.

A second type of boudinage is related to the occurrence of quartz pods in purely psammitic layers (Fig. 10). These quartz pods are organised in a fold train of the highly foliated psammites. The boudin axes have the same overall attitude as the fold hinges (~130/30). The quartz pods consistently occur in the northern limb of the N-verging, asymmetric fold train. Again, layer-parallel extension, giving rise to a series of foliation boudins and quartz pods in the boudin necks, clearly predates folding. The fabric of the quartz infill shows curved fibrous crystals with different internal growth surfaces, possibly indicating a brittle crack-seal origin of the foliation boudinage.

3.6 Structural domains

Based on the characteristic structural features of each outcrop, the outcrops can be grouped in five structural domains (Figs 4 & 11). Structural domain 1 is dominated by the primary cleavage (S_1), subparallel to bedding (S_0). No other foliations are apparent in rock sample nor in thin section. Rather thick layers of psammites are abundantly present. Structural domain 2 shows two visible foliations, the primary cleavage (S_1), dipping ~30° south, and the SBF (S_2), dipping ~10° south or oriented subhorizontal (Figs 5e, 6 & 7). This domain is characterised by an alternation of pelites, siltstones and psammites (Fig. 7). The latter rock type is most abundant. Structural domain 3 is characterised by the presence of the second type of chevron folds, i.e. folding the SBF (S_2), and its associated axial planar cleavage (S_3) (Figs 8b & 9). Contrary to domain 2, pelitic material is most abundant. Typical for structural domain 4 is the presence of the folded, finely laminated, multilayer sequence with characteristic pinch-and-swell structures of the individual psammitic layers (Figs 5c, d & 8a). Finally, structural domain 5 contains the folded foliation boudinage with quartz pods (Fig. 10). Both in structural domain 4 and 5 the tertiary cleavage (S_3) is axial planar with respect to the chevron folds (Fig. 5c & d).

The five structural domains identified are not randomly positioned (Fig. 4). A geometrical pattern has been recognised, enabling us to construct an overall geometrical model for the outcrop area (Fig. 11). The envelopes, that outline each structural domain, seem to follow the overall bedding attitude, i.e. dipping 30° south.

This suggests that the deformation did not affect the overall, regional bedding attitude. The geometrical model also suggests an increase of structural complexity towards the centre of the outcrop area, delimited at both northern and southern end by the structural domain 1. The outline of a high-strain zone, characterised by multiple foliation development, boudinage and chevron folding, becomes apparent.

4. Kinematic interpretation

A number of features presented in the structural analysis needs to be accounted for in whatever kinematic model put forward for the

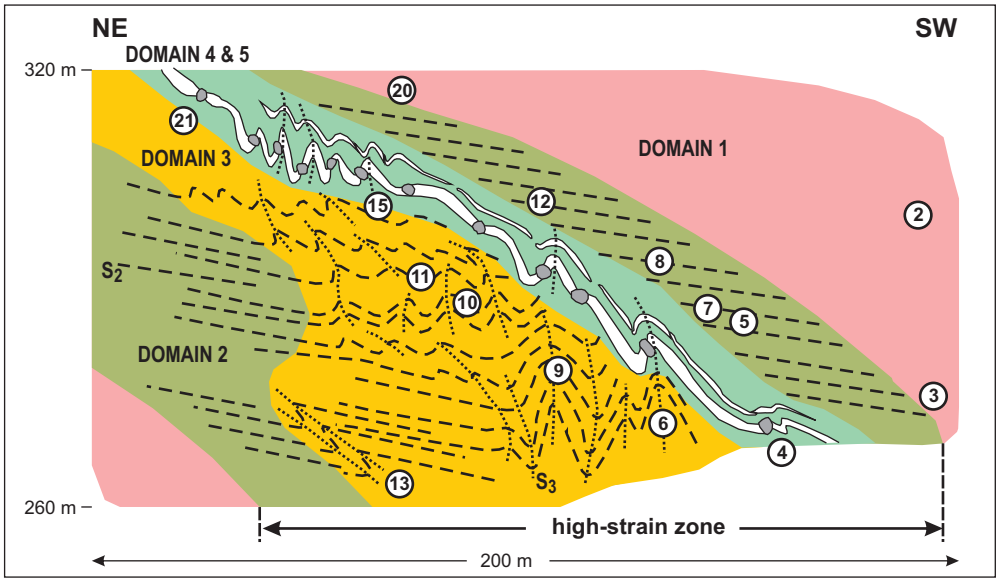

Figure 11. Geometrical model of the outcrop area (see figure 4 for location of the individual outcrops), outlining a high-strain zone. The outline of the different domains coincide with the overall bedding attitude, dipping ~30°S. White layers in structural domains 4 & 5 indicate folded, boudinaged layering; thick dashed lines indicate the SBF (S_2); thick dotted lines indicate the tertiary crenulation cleavage (S_3).

outcrop area:

- the bedding (S_0) can only be identified with certainty in the particular lithological context of finely laminated, psammite-pelite alternations; the main foliation throughout the outcrop area is the primary cleavage (S_1), which is consistently (sub-) parallel to the bedding;
- the primary fabric is affected by a multiple foliation development, a secondary shear band foliation (SBF = S_2) and a tertiary, axial planar, compressional crenulation cleavage (S_3); the presence of the different foliations is strongly lithology-dependent;
- different types of layer-parallel extension (i.e. boudinage) have occurred, predating folding;
- chevron folds developed on a pre-existing foliation – the primary foliation (S_1) or the secondary foliation (SBF = S_2) – and is associated with a tertiary, axial planar cleavage (S_3);
- the distribution of the different structural features is domainal; the domain envelopes express the overall regional bedding attitude; a strain gradient is present towards the central domain, outlining a high-strain zone.

Based on the kinematic interpretation of each of these particular structural features, an attempt is made to present an overall kinematic model, integrating the development of all structural features in one single, progressive deformation event.

4.1 Primary cleavage (sub-)parallel to bedding

Where observable in the finely laminated, psammite-pelite multilayers, the primary cleavage (S_1) makes a small angle (< 10°) to the bedding (S_0) (Fig. 5a). A tectonic origin is thus inferred for S_1. The apparent parallelism of primary cleavage and bedding is, moreover, a regional phenomenon in the entire central part of the Eifel depression (Van Baelen 2010).

This primary cleavage (S_1) is the tectonic foliation associated with the main stage of the Variscan orogeny in the High-Ardenne slate belt, i.e. the Sudetic stage (c. 320 Ma). This implies that this cleavage developed axial planar with respect to Variscan folds. In the High-Ardenne slate belt the typical N-verging fold trains are characterised by asymmetric folds with weakly S-dipping, long limbs and near-vertical to slightly overturned, short limbs (Fig. 12a). In folded multilayer sequences, the cleavage-bedding relationship shows a classical cleavage refraction pattern (Fig. 12a). The cleavage fabric is the most obvious in the more pelitic parts of the sequence (Fig. 12b).

The apparent parallelism of primary cleavage and bedding is therefore most probably not a primary feature. We consider the near-parallelism between cleavage and bedding as the result of a relative rotation of 'material planes' – both cleavage and bedding – towards mutual parallelism during a progressive, layer-parallel stretching. Both 'material planes' should be located in the extension (stretching) sector of the finite strain ellipsoid, representing the progressive strain accumulation (Fig. 12b & c).

Because no evidence is present to conclusively determine the younging direction of the rock sequence, two alternatives remain: a normal, weakly S-dipping limb or an overturned, steeply S-dipping limb in a N-verging, asymmetrical fold train. The alternative of the 'stretching', overturned short limb of a larger-scale, N-verging antiform is favoured in the light of our overall kinematic model that is presented below. During fold amplification – and related rotation – this limb is stretching parallel to bedding and flattening perpendicular to bedding, eventually giving rise to the near-parallelism between bedding and the primary cleavage (Fig. 12).

4.2 Shear band foliation

The primary cleavage fabric (S_1) was subsequently affected by the development of a weakly S-dipping to subhorizontal shear band foliation (SBF = S_2). This SBF consistently shows a top-to-the-north shear sense. The shear bands are relatively enriched in phyllosilicates and can be seen as cleavage domains (Fig. 5e), indicating fluid-assisted mass transfer (pressure solution creep) is the mechanism responsible for the development of the SBF.

With increasing shear-strain accumulation, the original bedding fabric has been drastically changed (Fig. 13). At first, the SBF caused the wavy appearance of the bedding fabric (Figs 6 &

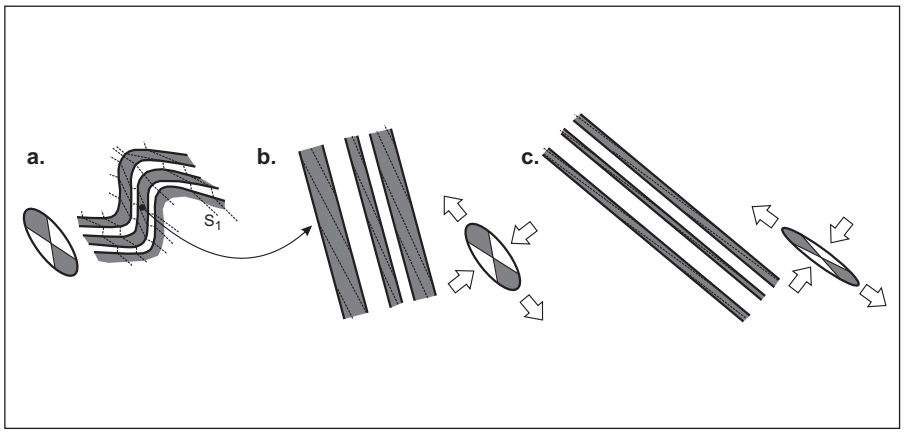

Figure 12. Conceptual kinematic model to explain the near-parallelism between bedding (S_0) and the primary cleavage (S_1). (a) cleavage refraction pattern in the steeply dipping, overturned short limb of a N-verging fold train with an overall S-dipping axial-planar cleavage (S_1). (b) detailed view of the overturned limb with a cleavage (dotted lines) present in the more pelitic parts of the multilayer sequence (gray shading). (c) detailed view of the stretched and rotated overturned limb with near-parallelism between bedding and primary cleavage. Corresponding finite strain ellipses are presented with extension (stretching) sectors in gray and contraction (flattening) sectors in white.

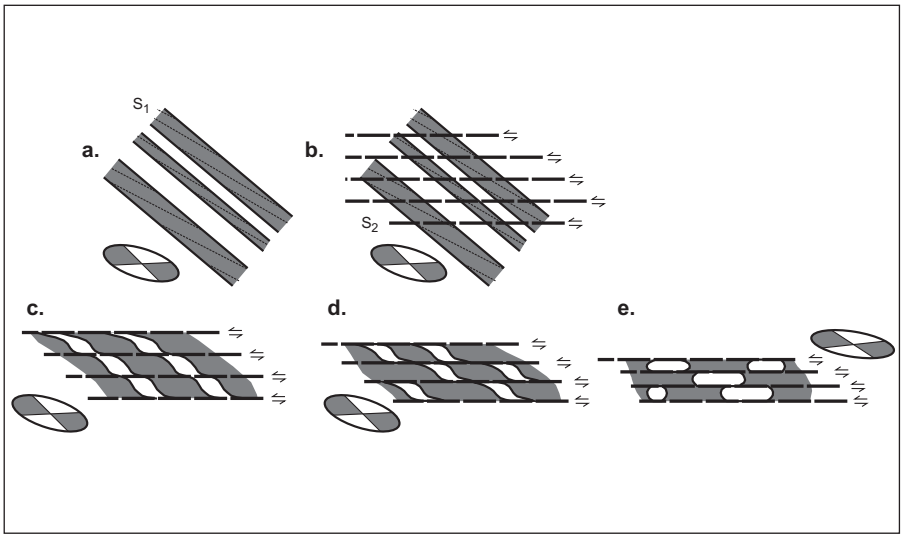

Figure 13. Conceptual kinematic model of the evolution of the shear band foliation (SBF = S_2). (a) starting position with the near-parallelism of bedding and primary cleavage (fine dotted lines). (b) development of extensional shear bands (thick dashed lines). (c) first stage of the protracted shear deformation, resulting in the wavy appearance of the bedding fabric (see figure 6). (d) second stage of the protracted shear deformation, resulting in the 'stretched fishes' (see figure 5e), typical for the 'swells' (see figure 14a). (e) final stage of the shear deformation, resulting in the complete transposition of the bedding by the SBF (T_{S0} // S_2) (see figures 5f & 9b), typical for the 'pinches' (see figure 14a). Corresponding finite strain ellipses are presented with extension (stretching) sectors in gray and contraction (flattening) sectors in white.

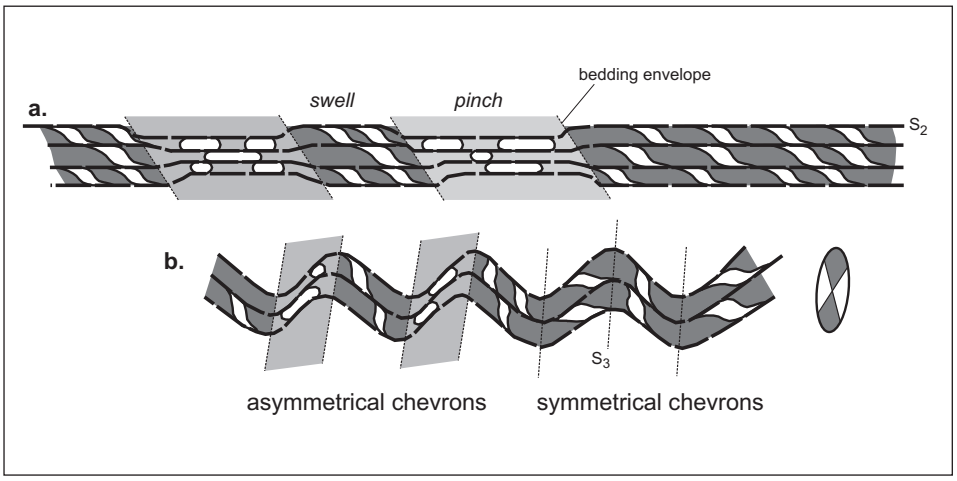

Figure 14. Conceptual kinematic model for the chevron folding of the SBF (S_2). (a) alternation of 'pinches' (light gray shading) and 'swells' (dark gray shading), related to lithological differences; the interface between both represents the overall bedding envelope. (b) subsequent chevron folding; asymmetric chevrons with limbs of variable thickness (see figures 8b & 9) develop on a pinch-and-swell sequence, while symmetric chevrons develop on a homogeneous swell sequence. Corresponding finite strain ellipse is presented with extension (stretching) sectors in gray and contraction (flattening) sectors in white.

13c). Ongoing shearing gave rise to the dismembering of the bedding, leaving 'stretched fishes' as a remnant of the original bedding fabric (Figs 5e & 13d). In the more pelitic horizons, increasing shear strain was accompanied by an extra flattening strain, perpendicular to the SBF. This heterogeneous strain accumulation eventually led to a complete transposition of the bedding fabric (T_{S0}), seemingly parallel to the SBF (Figs 5f, 9b & 13e). The result is an overall pinch-and-swell appearance of the SBF that can still be associated with the overall 'bedding envelope' (Fig. 14a). The development of the SBF introduced a new dominant anisotropy in the rock sequence. Moreover, the overall pinch-and-swell occurrence introduces a new mechanical heterogeneity that will exert a control on the subsequent deformation (Fig. 14).

The subhorizontal, top-to-the-north shearing was intimately linked to the progressive deformation of the stretched overturned limb, inferred from the near-parallelism of bedding and primary cleavage. The SBF accommodates the progressive rotation of the overturned limb in the overall top-to-the-north shearing, as well as the internal stretching of the limb. In this respect the SBF is similar to a C'-foliation in mylonites (Fig. 6) (Passchier & Trouw 2005, Trouw et al. 2010).

4.3 Boudinage

The finely laminated, psammitic layers in the predominantly pelitic multilayers clearly show pinch-and-swell structures, indicative for layer-parallel extension. This layer boudinage is consistent with the 'stretching' conditions within the progressively rotating overturned limb. The boudinage was thus coeval with the layer-perpendicular flattening leading to the near-parallelism between bedding and primary cleavage (Fig. 12).

In a homogeneous, well-foliated, psammite horizon, foliation boudinage caused the development of quartz pods (Fig. 10). The fibrous nature of the quartz infill indicates that crack-sealing is the active mechanism during a rather brittle fracturing of the psammite. Curved fibres suggest a limited rotational component to the extensional deformation, giving rise to the development of the quartz pods.

Finally, also the SBF shows a clear extensional component (see above), complying with the overall 'stretching' conditions present in the progressively rotating overturned limb.

4.4 Chevron folding

Shortening of the finely laminated, psammite-pelite series, affected by layer boudinage, first caused the imbrication and folding of the psammitic boudin fragments (Fig. 5b & c). Continuing shortening eventually gave rise to chevron folding of the multilayer sequence (Figs 5c & 8a). Associated with this shortening, an axial planar cleavage (S_3) developed, expressed in the pelitic horizons by a compressional crenulation cleavage (Fig. 5c & d).

Shortening of the psammitic package, in which foliation boudinage resulted in the presence of quartz pods, is expressed by flanking folds close to the quartz pods (Fig. 10). The asymmetry of the fold train, as well as the rotational component materialized in the curved fibrous infill of the quartz pods, infers a non-coaxial, top-to-the-north shear deformation causing the shortening..

The most striking folds are the chevron folds that affected the SBF (Figs 8b & 9). The development and progressive evolution of the SBF (S_2) (Fig. 13) and the associated pinch-and-swell occurrence (Fig. 14a) resulted in a heterogeneity in the rock sequence that controlled the subsequent folding (Fig. 14). The thin limbs of the chevron folds correspond to the 'pinches' with the transposed bedding fabric (T_{S0}) (Fig. 8b); the thick limbs to the 'swells' with the typical 'stretched fishes' (Fig. 8a). This suggests that the axial planes of these chevron folds coincide with lithological interfaces, i.e. the overall 'bedding envelope' (Fig. 14b). Folding caused locally a 'back-rotation' of this bedding envelope, antithetic with respect to the overall top-to-the-north shearing. While the asymmetric chevron folds developed in series dominated by pelitic material, more symmetric chevron folds developed in series dominated by psammitic material. In the latter folds, both limbs have the same thickness and show the internal fabric of the thick limbs of the asymmetric chevrons (Fig. 14b).

The contraction clearly occurred at the end of the progressive strain accumulation, postdating both boudinage and SBF development. On the basis of the observed asymmetry, we infer a top-to-the-north shear setting, suggesting chevron folding took place in the same context as the SBF development. In this overall top-to-the-north shear setting, 'material planes' rotated from the extension (stretching) sector of the incremental strain ellipsoid to the contraction sector. A rotation from extension to contraction sector is, however, not possible during a single progressive deformation event of homogeneous strain accummulation. It is therefore necessary that the overall strain context changed during the progressive shearing so that the 'material planes' – i.e. bedding and/or SBF – moved from the extension to the contraction sector.

4.5 Domainal configuration – bedding envelope & high-strain zone

A remarkable feature of the domainal configuration is the conservation of the regional bedding attitude in the envelopes outlining the different structural domains (Fig. 11). These 'bedding envelopes' appear not disturbed in the overall top-to-the-north shear setting, contrary to the high degree of polyphase, progressive deformation within each of the local domains. The deformation in each of the domains – both in extension and contraction – is eventually determined by their lithological characteristics.

We propose that these 'bedding envelopes' passively rotated during the progressive top-to-the-north shearing and associated stretching following a 'bookshelf model'. Within the domains, this 'bookshelf shearing' has been primarily accommodated by the development of the SBF (Fig. 15b).

The complex polyphase, progressive deformation is strongly localized in structural domains 2 to 5, outlining a 'high-strain zone' (Fig. 11). This high-strain zone is bordered at both sides by the structural domain 1, which is characterized by the presence of only the primary cleavage fabric (S_1) subparrallel to bedding (S_0). Consequently, structural domain 1 can be considered

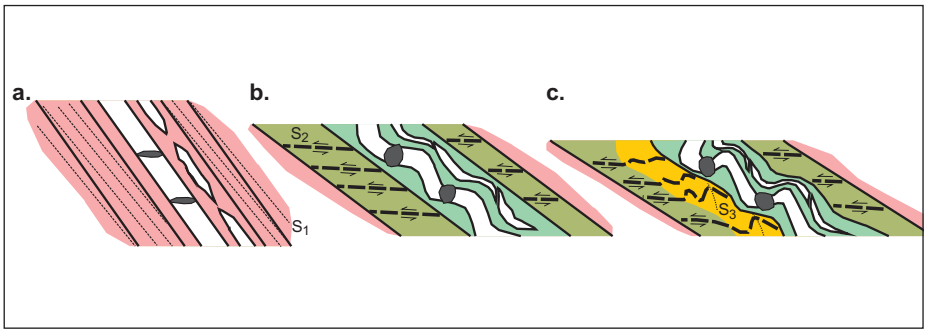

Figure 15. Conceptual kinematic model to explain the development of the structural domains in the high-strain zone. (a) first stage of the 'stretching' limb (= structural domain 1) (see figure 12). (b) development of SBF (S_2) (= structural domain 2) and initiation of folding (= structural domains 4 & 5). (c) chevron folding of SBF (S_2) and development of tertiary cleavage (S_3) (= structural domain 3). See figure 4 for colour code of the different structural domains.

as the 'protolith' in which the high-strain zone developed. Strain localisation is most probably due to particular lithological properties that influence the mechanical variation within the rock sequence. The high-strain zone materializes a progressive, non-coaxial shear deformation with a consistent top-to-the-north shear sense. In other words, this high-strain zone is a ductile shear zone.

4.6 Kinematic model

The presence of a primary cleavage (S_1) at an angle to bedding (S_0) infers a – Sudetic – folding stage, in which the primary cleavage develops axial planar to the folds. Based on the overall, weakly to moderately, S-dipping attitude of the primary cleavage a N-verging fold train is inferred. Taking into account the overall weakly S-dipping to subhorizontal fold envelope, characterizing the High-Ardenne slate belt (Asselberghs 1946), the N-verging fold train most probably consists of long, weakly S-dipping, normal limbs alternating with short, strongly north- ('normal') to S-dipping ('overturned') limbs. The weakly S-dipping, axial planar cleavage (~30°S) suggests that the short limbs are most probably overturned (Fig. 16b).

We have interpreted the small angle between the primary cleavage and the bedding as the result of a rotation of both 'material planes' towards mutual parallelism within a 'stretching and thinning' fold limb. This fold limb, exposed in the outcrop area, is thus situated in the extension sector of the bulk finite strain ellipsoid. This is corroborated by the layer and foliation boudinage, inferring layer-parallel extension. Although no conclusive evidence has been found to determine the stratigraphic facing, we assume that the outcrop area is located in the overturned short limb of a N-verging fold train (Fig. 16b).

Progressive fold amplification induces further rotation of the 'stretching and thinning' limb in this overall non-coaxial strain setting. This non-coaxial strain exerted on a highly anisotropic rock sequence (because of the near-parallelism of the primary cleavage and bedding) resulted in the development of extensional shear bands at a small angle to the dominant anisotropy (cf. Passchier & Trouw 2005). The development of this shear band foliation (SBF = S_2) accommodated not only further stretching and thinning (Fig. 16c) but also the passive rotation of the limb (cf. 'bookshelf model') (Fig. 15). Rotation of the quartz pods and associated development of flanking folds may be initiated at this stage (Fig. 15b). Protracted shearing promotes strain localization, giving rise to a high-strain zone (Fig. 16d).

In the final stage the overall strain accumulation changed from extension-dominated to contraction-dominated, as expressed by the chevron folding of both bedding and SBF (Fig. 15b & c). These late, shear-related folds (cf. Carreras et al. 2005) are associated with the development of a compressional crenulation cleavage (S_3) of both the primary (S_1) and secondary foliation (S_2) in the chevron folds affecting both bedding and SBF, respectively (Figs 15c & 16e). The change of overall strain accumulation – from extension- to contraction-dominated – within the thinned and stretched, overturned limb is most probably caused by the change in dominant mechanical anisotropy. The SBF indeed becomes the dominant 'material plane' in the rock sequence. This material plane, weakly S-dipping to horizontal, is located in the contraction sector of the incremental strain ellipsoid.

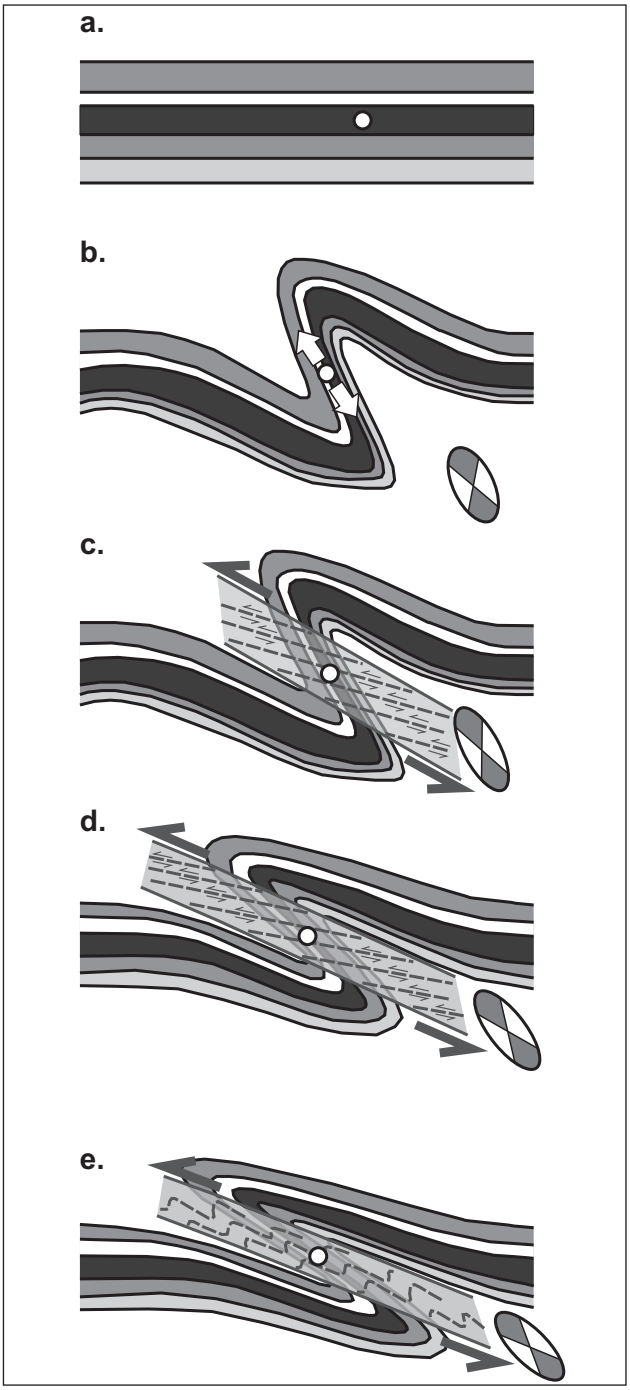

Figure 16. Conceptual kinematic model for the development of the 'Herbeumont shear zone' (white circle indicates study area). (a) initial context of multilayer sequence. (b) development of an N-verging, asymmetric fold with a 'stretching and thinning' overturned short limb. (c) fold amplification accommodated by the development of SBF, localized in a 'high-strain zone' (gray shading). (d) protracted strain localization, giving rise to the development of a top-to-the-north 'shear zone'. (e) chevron folding of SBF, due to a shift of extension-dominated tot contraction-dominated deformation.

5. Discussion

An overall kinematic model has been proposed that consistently explains all structural features observed, including the multiple foliations, the boudin structures and the chevron folds. A shear-related, high-strain zone in an overall top-to-the-north shear setting has been identified. The three stages of the polyphase, progressive deformation reveals a change from extension-dominated (stages 1 & 2) (Fig. 16b to d) to contraction-dominated strain accumulation (stage 3) (Fig. 16e). A number of questions remain unanswered, however, in particular with respect to the regional context of the kinematic model. In addition, the applicability to other parts of the High-Ardenne slate belt still needs to be validated.

5.1 'Herbeumont shear zone'

A ductile shear zone, some 100 m wide, has been identified in the outcrop area on the east bank of the Semois river, just northwest of the Herbeumont castle (Fig. 11). We define the 'Herbeumont shear zone' to identify the shear-related, high-strain zone passing the outcrop area. We consider this ductile shear zone primarily as a 'stretched and thinned' overturned, short limb belonging to a N-verging, fold train. We believe that the 'Herbeumont shear zone' does not have a significant amount of displacement and should definitively not be seen as a major thrust. The stratigraphic context, exposing the same lithostratigraphical formation in both footwall and hanging wall, confirms this assumption. Following our kinematic model, the 'Herbeumont shear zone' may have developed in the stretched and thinned, overturned northern limb of the Givonne culmination (Figs 2 & 16). The question then needs to be asked if the characteristic features of the 'Herbeumont shear zone' are also present at the other outcrop areas of the 'Herbeumont fault'.

Projecting the trace of the 'Herbeumont shear zone' to the east, it crosses the railway section some 100 m south of the type locality of the 'Herbeumont fault' (Fig. 3). In the original descriptions (Asselberghs 1946, Fourmarier 1914) no indications can be found, however, of any significant disturbance in that part of the railway section. Moreover, the current condition of the railway section does not allow to check whether or not a high-strain zone could be identified. It is, therefore, fair to assume that the 'Herbeumont shear zone', as identified on the east bank of the Semois river, should continue towards the 'Herbeumont fault', as described in the railway section. The description of structural features in the railway section by Asselberghs (1946) (see above), which are rather comparable with our observations, supports this hypothesis.

An individual fault or fault zone has not been observed on the east bank of the Semois river. We can, though, not exclude the existence of a brittle fault – the 'Herbeumont fault' – completing the deformation history as outlined in our kinematic model.

5.2 Regional context

The entire central part of the Eifel depression in the Herbeumont-Cugnon area is characterised by near-parallelism of primary cleavage and bedding. We interpreted this near-parallelism as a secondary feature caused by the stretching and thinning – and the related rotation of 'material planes' – within an overturned short limb, situated in the extension sector of the overall finite strain ellipsoid (Fig. 12). We may thus speculate that the entire central part of the Eifel depression consists of a stretched and thinned, overturned limb. Shear-related high-strain zones, such as the 'Herbeumont shear zone', should be rather common in such a context. The presence of a SBF on outcrops north of Herbeumont corroborates this idea (Van Baelen 2010). In addition to looking for evidence of shear, one should specifically look for the normal limb of this fold train, in which primary cleavage and bedding are expected to be clearly discernable at a relatively high angle to each other. Most probably, this 'normal' context would not allow any shear strain localization because of the lack of a pervasive mechanical anisotropy (i.e. near-parallelism of bedding and primary cleavage) (see also Van Baelen & Sintubin, 2008).

In the Herbeumont-Cugnon area another intriguing tectonic feature is exposed in the footwall of the 'Herbeumont shear zone'. Recent studies revealed late, extensional detachment zones with a clear top-to-the-south shear sense (Van Baelen 2010). These detachment zones affect the primary cleavage fabric, and in that respect are very comparable to the inferred kinematics in the 'Herbeumont shear zone'. Both are relative late with respect to the main stage of the Variscan deformation in the High-Ardenne slate belt. However, the kinematic, as well as temporal, relationship between the top-to-the-north 'Herbeumont shear zone' and the top-to-the-south detachment zones remains enigmatic. It cannot be excluded, however, that both features materialize different aspect of the same overall deformation event at the latest stages of the Variscan orogeny (cf. Druguet et al. 2009).

5.3 A cautionary note

The different types of chevron folds holds a warning for those performing fieldwork in slate belts, in particular when the original bedding fabric is hard to identify. The shear band foliation in the chevron folds can easily be mistaken for bedding (Figs 8 & 9). The thickness variation (Fig. 8) can also be considered suspicious, leading to an alternative interpretation such as cleavage refraction, thus identifying the bedding with the axial planes of the chevron folds. Only the thin sections revealed the true nature of the apparent bedding in these chevron folds, i.e. a shear band foliation affecting the primary cleavage/bedding fabric.

On the other hand, we recognized four different planar features: bedding, primary cleavage, shear band foliation and the tertiary crenulation cleavage. What the outcrops learned, is that the presence of a foliation largely depends on the local lithological characteristics. It is, therefore, imperative that the question which foliations are present, is asked again at each individual outcrop.

6. Conclusions

The outcrop area along the banks of the Semois river at Herbeumont offers an excellent opportunity to look into a shear zone that developed in low-grade metamorphic conditions in a slate belt. In an overall top-to-the-north shear setting, a polyphase, progressive strain accumulation resulted in a complex superposition of structural features, such as multiple foliations, boudin structures and chevron folds. The near-parallelism of the primary cleavage and bedding, together with the boudinage, is explained by a stretching and thinning of the rock sequence, of which the main anisotropy – i.e. bedding and primary cleavage – is situated in the extension sector of the incremental strain ellipsoid related to the shearing. Non-coaxial strain accumulation is subsequently expressed by the development of a shear band foliation, accommodating the overall top-to-the-north shear component. Finally, late, shear-related folds indicate a change in strain accumulation from extension-dominated to contraction-dominated. The mechanical properties of the newly developed shear band foliation may have caused this kinematic switch. Eventually, no brittle deformation – i.e. thrust fault development – has been observed. In a slate belt, the presence of multiple foliations not necessarily mean that multiple orogenic events affected the rock sequence. As demonstrated in our kinematic analysis, the development of multiple foliations can easily be framed in one single, progressive strain accumulation, belonging to one single orogenic event. The way strain is accumulated, is mainly controlled by the changing mechanical properties of the rock sequence, expressed in slate belts primarily by planar anisotropies. In our case, the controlling anisotropy shifted from a lithology-dependent anisotropy, i.e. bedding, to a tectonically induced anisotropy, i.e. the shear band foliation. This complex superposition of multiple foliations characterised the central part of the Eifel depression. In the poorly exposed High-Ardenne slate belt, multiple foliations may thus serve as a 'proxy' to identify high-strain zones.

The development of the 'Herbeumont shear zone' fits in a continuum of a long-lasting deformation history that is recorded in the High-Ardenne slate belt. The entire deformation history seems to have occurred under very similar mid-crustal brittle-ductile conditions. The onset of the orogeny is expressed by extensive quartz veining (Kenis et al. 2005a, Kenis & Sintubin 2007, Kenis et al. 2002, Van Noten et al. 2008, Van Noten & Sintubin 2010), followed by a layer-parallel shortening event

(Kenis et al. 2005b, Kenis et al. 2004, Urai et al. 2001). The main stage of the orogeny is characterised by the development of N-verging, fold trains and the associated pervasive, primary slaty cleavage, becoming the dominant anisotropy controlling the subsequent deformation in the slate belt. Late stages of the deformation history are recorded in shear-related, high-strain zones, such as the 'Herbeumont shear zone' discussed in this paper, as well as in brittle-ductile extensional detachment zones (Van Baelen 2010).

7. Acknowledgments

The research of Yvonne Schavemaker at the K.U.Leuven was made possible in the framework of the Lifelong Learning Programme – Erasmus of the European Commission. Manuel Sintubin is Research Professor of the Onderzoeksfonds – K.U.Leuven. This paper frames in the symposium 'Tectonics and Structural Geology in Belgium' (Contact Forum Académie Royale des Sciences, des Lettres et des Beaux-Arts de Belgique, Brussels, 14 May 2010).

The authors thanks the reviewers, Timothy Debacker and Olivier Bolle, for their detailed comments, which definitively helped improving the paper.

8. References

Asselberghs, E., 1922. Compte Rendu de la Session Extraordinaire de la Société Géologique de Belgique tenue à Bertrix les 25, 26 et 27 septembre 1921 dans le Siegenien du Synclinal de l'Eifel. Annales de la Société géologique de Belgique, 44, B207-B228.

Asselberghs, E., 1946. L'Eodévonien de l'Ardenne et des régions voisines. Mémoires de l'Institut géologique de l'Université de Louvain, 14, 1-598.

Belanger, I., 1998. Effets d'une déformation hétérogène sur un ensemble mécaniquement anisotrope: le cas du Massif de Rocroi (Ardenne franco-belge). Unpublished Ph. D. thesis, Université Catholique de Louvain.

Berthé, D., Choukroune, P. & Gapais, D., 1979. Orientations préférentielles du quartz et orthogneissification progressive en régime cissaillant: l'exemple du cisaillement sud-armoricain. Bulletin de Minéralogie, 102((2-2)), 265-272.

Beugnies, A., 1986. Le métamorphisme de l'aire anticlinale de l'Ardenne. Hercynica, 2(1), 17-33.

Bultynck, P. & Dejonghe, L., 2001. Devonian lithostratigraphic units (Belgium). Geologica Belgica, 4(1-2), 39-69.

Carreras, J., Druguet, E. & Griera, A., 2005. Shear zone-related folds. Journal of Structural Geology, 27, 1229-1251.

Delvaux de Fenffe, D. & Laduron, D., 1984. Analyse structural au bord sud du Massif de Rocroi (Ardennes françaises). Bulletin de la Société belge de Géologie, 93, 11-26.

Delvaux de Fenffe, D. & Laduron, D., 1991. Caledonian and Variscan structures in the Rocroi-Ardenne Lower Paleozoic basement (Belgium and adjacent countries). Annales de la Société géologique de Belgique, 114, 141-162.

Druguet, E., Alsop, G. I. & Carreras, J., 2009. Coeval brittle and ductile structures associated with extreme deformation partitioning in a multilayer sequence. Journal of Structural Geology, 31(5), 498-511.

Fielitz, W. & Mansy, J.-L., 1999. Pre- and synorogenic burial metamorphism in the Ardenne and neighbouring areas (Rhenohercynian zone, central European Variscides). Tectonophysics, 309, 227-256.

Fourmarier, P., 1914. Observations sur le versant Nord et al partie centrale du synclinal de l'Eifel dans la région de Bertrix-Herbeumont. Annales de la Société géologique de Belgique, 41, B323-B330.

Fourmarier, P., 1944. Une anomalie de la schistosité dans le Dévonien de la Semois. Annales de la Société géologique de Belgique, 67, B29-B36.

Fourmarier, P., 1966. Remarques à propos de petits plis en chevron et de leur signification en tectogénèse. Annales de la Société géologique de Belgique, 89, 33-44.

Fourmarier, P., Bintz, J., Lambrecht, L. & Heyart, H., 1968. Anomalies de la schistosité dans le Paléozoique de la Haute-Ardenne. Annales de la Société géologique de Belgique, 91, 171-269.

Geukens, F., 1969. De ouderdom der druksplijting in het Caledonische Massief van Stavelot. Mededelingen van de Koninklijke Academie voor Wetenschappen, Letteren en Schone Kunsten van België, Klasse der Wetenschappen, 31(4), 1-13.

Godefroid, J., Blieck, A., Bultynck, P., Dejonghe, L., Gerrienne, P., Hance, L., Meilliez, F., Stainier, P. & Steemans, P., 1994. Les formations du Dévonien Inférieur du Massif de la Vesdre, de la fenêtre de Theux et du Synclinorium de Dinant (Belgique, France). Mémoires pour servir à l'explication des Cartes géologiques et minières de la Belgique, 38, 1-144.

Gosselet, J., 1888. L'Ardenne. Mém. Expl. Carte géol. France, 1-889.

Kenis, I., Muchez, P., Verhaert, G., Boyce, A. J. & Sintubin, M., 2005a. Fluid evolution during burial and Variscan deformation in the Lower Devonian rocks of the High-Ardenne slate belt (Belgium): sources and causes of high-salinity and C-O-H-N fluids. Contribution to Mineralogy and Petrology ,150, 102-118.

Kenis, I. & Sintubin, M., 2007. About boudins and mullions in the Ardenne-Eifel area (Belgium, Germany). Geologica Belgica, 10(1-2), 79-91.

Kenis, I., Sintubin, M., Muchez, P. & Burke, E. A. J., 2002. The "boudinage" question in the High-Ardenne slate belt (Belgium): a combined structural and fluid inclusions approach. Tectonophysics, 348, 93-110.

Kenis, I., Urai, J. L., van der Zee, W., Hilgers, C. & Sintubin, M., 2005b. Rheology of fine-grained siliciclastic rocks in the middle crust - evidence from structural and numerical analysis. Earth and Planetary Science Letters, 233, 351-360.

Kenis, I., Urai, J. L., van der Zee, W. & Sintubin, M., 2004. Mullions in the High-Ardenne Slate Belt (Belgium). Numerical model and Parameter Sensitivity Analysis. Journal of Structural Geology, 26(9), 1677-1692.

Oncken, O., von Winterfeld, C. & Dittmar, U., 1999. Accretion of a rifted passive margin: The Late Paleozoic Rhenohercynian fold and thrust belt (Middle European Variscides). Tectonics, 18(1), 75-91.

Passchier, C. W. & Trouw, R. A. J., 2005. Microtectonics. Springer-Verlag, Berlin.

Piessens, K. & Sintubin, M., 1997. Partitioning of Variscan strain in the southern part of the Caledonian Stavelot-Venn Inlier in the Ardenne Allochthon (Belgium). Aardkundige Mededelingen, 8, 135-138.

Piqué, A., Huon, S. & Clauer, N., 1984. La schistosité hercynienne et le métamorphisme associé dans la vallée de la Meuse, entre Charleville-Mézières et Namur (Ardennes franco-belges). Bulletin de la Société belge de Géologie, 93(1-2), 55-70.

Platt, J. P. & Vissers, R. L. M., 1980. Extensional structures in anisotropic rocks. Journal of Structural Geology, 2(4), 397-410.

Rondeel, H. E., 1971. About three sets of kink bands near Herbeumont (Belgian Ardennes). Geologische Rundschau, 60(3), 912-923.

Sintubin, M., Debacker, T. N. & Van Baelen, H., 2009. Early Palaeozoic orogenic events north of the Rheic suture (Brabant, Ardenne): A review. Comptes Rendus Geoscience, 341, 156-173.

Trouw, R., Passchier, C. W. & Wiersma, D. J., 2010. Atlas of Mylonites - and related microstructures. Springer-Verlag, Berlin.

Urai, J. L., Spaeth, G., van der Zee, W. & Hilgers, C., 2001. Evolution of mullion (formerly boudin) structures in the Variscan of the Ardennes and Eifel. Journal of the Virtual Explorer, 3, 1-15.

Van Baelen, H., 2010. Dynamics of a progressive vein development during the late-orogenic mixed brittle-ductile destabilisation of a slate belt. Examples of the High-Ardenne slate belt (Herbeumont, Belgium). Aardkundige Mededelingen, 24, 1-221.

Van Baelen, H. & Sintubin, M., 2008. Kinematic consequences of an angular unconformity in simple shear: an example from the southern border of the Lower Palaeozoic Rocroi inlier (Naux, France). Bulletin de la Société géologique de France, 179(1), 73-87.

Van Noten, K., Hilgers, C., Urai, J. L. & Sintubin, M., 2008. Late burial to early tectonic quartz veins in the periphery of the High-Ardenne slate belt (Rursee, North Eifel, Germany). Geologica Belgica, 11(3-4), 179-198.

Van Noten, K. & Sintubin, M., 2010. Linear to non-linear relationship between vein spacing and layer thickness in centimetre- to decimetre-scale siliciclastic multilayers from the High-Ardenne slate belt (Belgium, Germany). Journal of Structural Geology, 32(3), 377-391.

Verniers, J., Pharaoh, T. C., André, L., Debacker, T. N., De Vos, W., Everaerts, M., Herbosch, A., Samuelsson, J., Sintubin, M. & Vecoli, M., 2002. The Cambrian to mid Devonian basin development and deformation history of eastern Avalonia, east of the Midlands Microcraton: new data and a review. In: Palaeozoic Amalgamation of Central Europe (edited by Winchester, J. A., Pharaoh, T. C. & Verniers, J.). Special Publications, 201. Geological Society, London, 49-93.

Manuscript received 01.08.2011, accepted in revised form 23.01.2012, available on line 15.02.2012